In-flight measurements of lightning locations using an aircraft-mounted lightning mapper

Milani, Zachary; Nichman, Leonid; Matida, Edgar; Fleury, Liam; Wolde, Mengistu; Bruning, Eric; McFarquhar, Greg M.; Kollias, Pavlos

Publisher’s version / Version de l'éditeur:

https://doi.org/10.1016/j.ast.2025.110038

Aerospace Science and Technology, 160, pp. 1-10, 2025-02-07

Aerospace Science and Technology 160 (2025) 110038

Contents lists available at ScienceDirect

Aerospace Science and Technology

journal homepage: www.elsevier.com/locate/aescte

In-flight measurements of lightning locations using an aircraft-mounted lightning mapper

Zachary Milani [a,b,*], Leonid Nichman [a,b], Edgar Matida [a], Liam Fleury [b], Mengistu Wolde [b], Eric Bruning [c], Greg M. McFarquhar [d], Pavlos Kollias [e]

[a] Carleton University, Ottawa, ON, K1S 5B6, Canada
[b] National Research Council of Canada, Ottawa, ON, K1V 1J8, Canada
[c] Texas Tech University, Lubbock, TX 79409-1053, USA
[d] Cooperative Institute for Severe and High Impact Weather Research and Operations (CIWRO) and School of Meteorology, University of Oklahoma, Norman, OK 73072-7304, USA
[e] Stony Brook University, Stony Brook, NY 11794-5000, USA

A R T I C L E I N F O

Communicated by: Dr Mehdi Ghoreyshi

Keywords:
Lightning detection
Dangerous weather
Airborne measurement
Flight safety
Decision aid

A B S T R A C T

Real-time measurements of lightning locations can improve flight safety by providing aircraft operators with valuable information about nearby weather conditions. Lightning warnings can be especially valuable when piloting aircraft that are more susceptible to a direct strike such as electric aircraft, hydrogen-powered aircraft, and even UAVs with composite skins. At best, weather updates are broadcast from weather services every 2.5 to 5 mins, but it's not uncommon for an intermittent connection to cause service stability issues. Therefore, an aircraft-mounted lightning mapper might be the most practical source of real-time lightning information for pilots. This work investigates the in-flight performance of the aircraft-mounted Stormscope Weather Mapping System (WX-500 Series 2) through comparisons to the Houston Lightning Mapping Array, National Lightning Detection Network, and the GOES - Geostationary Lightning Mapper. Measurements from two thunderstorms near Houston, TX, yielded WX-500 detection efficiencies of 33 % and 42 % for intracloud flashes, 75 % and 64 % for cloud to ground flashes, and 53 % and 79 % for total flashes. The WX-500 bearing measurement was accurate to within $\pm 14^\circ$ (σ), which improved to $\pm 4^\circ$ when integration time was increased from 2 to 30 s and clear outliers were ignored. The WX-500 range measurement was overestimated by an average of +74 km ($\pm$50 km) when the average true flash distance was 94 km. The WX-500 accurately depicted the boundary of lightning activity at an integration time of 1 min which is sufficient for the circumnavigation of thunderstorms.

1. Introduction

Lightning poses a significant risk to aircraft safety, especially as the aviation industry transitions from conventional to hybrid, electric, and composite material aircraft [1–4]. Everyday aerial activities like personal or public transportation and the delivery of goods will become increasingly dependent upon vehicles like remotely piloted aircraft systems (RPAS), unmanned aerial vehicles (UAVs), and vertical take-off and landing aircraft (VTOLs). Innovative electric and hydrogen aircraft are uniquely vulnerable to direct lightning strikes and will require rigorous certification and flight operation standards to prevent significant damage from a direct lightning strike. Incidents in which lightning penetrates through the skin of conventional aircraft are indicative of the challenges associated with developing and testing safety standards that protect against unpredictable and violent atmospheric electrical discharges [5,6]. In addition to electrical discharges, lightning-producing clouds may exhibit strong wind shear, powerful convective updrafts, heavy precipitation, and an abundance of ice hydrometeors which should be avoided for a safe and comfortable flight [7,8]. An aircraft-mounted, real-time, lightning mapper can be an extremely effective navigational tool for detecting and avoiding electrically active clouds thereby reducing the risk of a direct strike and experiencing dangerous flight conditions.

Given that pilots rely on their personal interpretation of radar products from on-board weather radar, additional information about lightning type, location, and flash rate, can help to infer different cloud

* Corresponding author.
E-mail address: zacharymilani@cmail.carleton.ca (Z. Milani).

https://doi.org/10.1016/j.ast.2025.110038
Received 1 October 2024; Received in revised form 5 February 2025; Accepted 6 February 2025
Available online 7 February 2025

processes and gain a more complete understanding of weather conditions. Access to weather and lightning data streams is available through paid subscription services like SiriusXM Aviation which has an industry leading update rate of (at best) 2.5 mins, or through free services like ADS-B which updates every 5 mins [9]. These streaming services are convenient and very useful, but they require a stable uplink connection, and their availability is limited to select regions which makes them more valuable for flight planning than in-flight navigation (e.g., SiriusXM Aviation coverage is limited to the CONUS and Southern Canada). For instance, an individual thunderstorm cell can be on the order of 15 km in diameter with an average lifetime of 30 to 60 mins and a commercial turbofan aircraft travelling at 200 m/s can cover roughly 34 km in-between weather updates that refresh every 2.5 min [10]. The airborne lightning mapper will show lightning locations in real-time allowing pilots to make important navigational decisions without the hesitation of waiting for the next weather update.

The airborne lightning mapper is a compact and lightweight cross-loop antenna mounted to the outer surface of an aircraft whose data is processed by an on-board processing unit that maps lightning activity relative to aircraft position and heading on a flight deck display. The Stormscope is claimed to be the most popular lightning mapper for the general aviation market having sold over 80,000 units as of 2019 [11]. Other commercially available systems include the LSZ-850/860 [12], the Insight Strikefinder [13] and the Avidyne TWX670. Airborne lightning mappers are particularly popular in areas known to have frequent and intense thunderstorms (e.g., the coastal areas of Florida) and can be the only source of on-board weather data on aircraft without a bulky forward-facing radar system. While the benefits of real-time lightning measurements are clear, widespread commercial use of the airborne lightning mapper likely stalled because early models were qualitative and imprecise during a time when doppler weather radar technology was being developed for thunderstorm identification (circa 1980s) [14], and the National Lightning Detection Network was providing lightning strike locations over North America to within 10 km (circa 1988) [15].

The literature on airborne lightning mappers that include in-flight data is limited to government reports from the 1980s, investigating the original Ryan Stormscope or the original LSZ-850 (See S.I. Table 1 for literature summary). The literature shows how individual strikes measured by the Ryan Stormscope align poorly with the flashes measured by the ground-based lightning mapping networks [16]. Furthermore, Ryan Stormscope detections were typically poorly clustered and dispersed significantly in the radial direction and slightly in the bearing direction [16,17]. Since these findings were published, newer models, such as the WX-500, have been developed to include advanced signal processing techniques and strike clustering algorithms. For instance, the WX-500 storm cell detection algorithm called "Cell mode" modifies the original location of individual strikes and clusters them around the expected thunderstorm cell location. Although the WX-500 is claimed to have several additional upgrades over its predecessors (e.g., see end of S.I. Section 3) there is no quantitative analysis of its performance beyond the limited information provided by the original manufacturer.

This study aims to fill the gap in the literature on the modern airborne lightning mapper by investigating the in-flight performance of the aircraft-mounted Stormscope Weather Mapping System (WX-500 Series 2). A WX-500 was installed on the Convair-580 research aircraft owned and operated by the National Research Council of Canada (NRC) [18] during the Experiment of Sea Breeze Convection, Aerosols, Precipitation, and Environment (ESCAPE) [19] campaign in Houston, Texas, which targeted and observed convective updrafts (up to 30 m/s) and ran from May to June in 2022. This work investigates the only two flights with significant thunderstorm activity during the campaign and compares the WX-500 to collocated lightning measurements from the Houston Lightning Mapping Array, National Lightning Detection Network, and the GOES - Geostationary Lightning Mapper. The objectives of this work include: i) estimate the WX-500 detection efficiency for different flash types; ii) review WX-500 flash rate and factors that affect lightning detection; iii) estimate WX-500 bearing and range accuracy; iv) investigate bearing span and how it can be used as a navigational aid; and v) identify future work that can improve upon the deficiencies of the modern airborne lightning mapper.

2. Methods

2.1. Lightning mappers

The WX-500 consists of an antenna, processor unit, and display. The WX-500 antenna is a NY-163 flat-pack antenna (P/N 805–10,930–001) that was mounted to the belly of the NRC Convair-580, along its centerline and 14.2 m back from the nose. The exact mounting location of the WX-500 antenna is shown in S.I. Fig. 1. The WX-500 antenna measures the electromagnetic pulse-like signal emitted from a lightning discharge using two orthogonal loop antennas and a 'sense' antenna to account for 180-degree ambiguity inherent to this type of measurement [16]. The WX-500 calculates the range (distance to signal origin) and bearing (azimuth of signal origin relative to aircraft heading) of lightning activity using single-station magnetic direction-finding (DF) techniques (see S.I. Section 3 for more details). The WX-500 is sensitive to VLF signals with an estimated working range of at least 3 to 120 KHz [20,21]. The WX-500 can detect lightning up to 370 km in all directions [22]. The WX-500 processor (P/N 805–11,500–001) was located inside the fuselage and an Apollo MX20 multi-function display located on the flight deck displayed the processed data.

The WX-500 does not distinguish between when a waveform is produced by a lightning 'event' or 'flash' (events are the many discrete discharges that make up a flash). Therefore, an individual WX-500 data point is a general measurement of lightning activity and for simplicity is referred to as a "strike". A WX-500 strike cannot be directly linked to a single event, nor can it be directly linked to a single flash when two flashes have occurred. All WX-500 strikes are processed and reported at 2 s intervals. Each report that was sent by the WX-500 processor to the multi-function display was also recorded by the NRC Convair-580 data logger, which tagged the report with the time it was received.

The Houston Lightning Mapping Array (HLMA) is a ground network of more than twelve VHF sensors (60 to 66 MHz) located in and around the Greater Houston Area. The HLMA maps the 3-D location (i.e., latitude, longitude, altitude) of lightning channels in real-time using time of arrival (TOA) geolocation and provides estimates of flash-level properties like power and volume [23]. The HLMA detects nearly 90 % of flashes within a 300 km radius of its centroid location (29.76°N, 95.37°W) [23,24]. The HLMA can measure individual lightning events with a temporal accuracy of $\pm$25 ns [25] and spatial accuracy within $\pm$20 m [23,26]. Flash data from the HLMA collected during ESCAPE [24, 27] are used as the ground truth measurement of total lightning activity. While the HLMA excels at mapping lightning channels through the atmosphere, it cannot easily identify the type of flash that was emitted.

The National Lightning Detection Network (NLDN) is a ground network with over one-hundred-and-fourteen LS7002 sensors spread across North America which monitor lightning activity in real-time over Canada and the United States [28,29]. The network uses a combination of DF (like the WX-500) and TOA techniques to map lightning discharges in 2D with an expected accuracy of between 200 and 300 m in the interior network [28]. This uncertainty is roughly equivalent to 0.2° of bearing error when measuring a flash from around 100 km away using a single-station sensor like the WX-500. The NLDN can differentiate between the return strokes that define a cloud to ground flash (CG flash) and the atmospheric discharges that define an intracloud flash (IC flash). The NLDN classification accuracy for CG flashes is estimated to be 96 % (i.e., 4 % of return strokes are misclassified as IC discharges) [30]. The NLDN detection efficiency was estimated to be between 30 % and 58 % for pure IC flashes [29] and upwards of 92 % to 94 % for CG flashes [30, 31]. Return strokes identified by NLDN data were used to classify HLMA and GOES-GLM data as either CG or IC flashes.

The Geostationary Operational Environmental Satellite (GOES-16) includes a Geostationary Lightning Mapper (GLM), an optical camera that measures the line-of-sight intensity of lightning emission at a wavelength of 777 nm [32]. The GOES-GLM has a frame rate of 2 ms and a 2D spatial mapping accuracy of <8 km over North America [32]. Since the GOES-GLM is an optical measurement and the ground networks measure radio frequencies, they do not necessarily detect the same components of a lightning flash [33]. However, the GOES-GLM was determined to detect 87 % of CG flashes that were coincidently measured by the lightning mapping array at Kennedy Space Center and by the NLDN [33]. Moreover, the GOES-GLM detects up to 40 % of small and short-duration flashes and upwards of 95 % for strong and long-duration flashes [33]. Data from the GOES-GLM [34] are primarily used to determine overlap between the coverage areas of the WX-500 and HLMA and are carefully used for WX-500 validation in the absence of HLMA data.

2.2. Data acquisition during the ESCAPE campaign

Airborne lightning data were collected during the ESCAPE campaign by the NRC Convair-580 research aircraft, which was also tasked with measuring several different properties of convective clouds. Potential storms were selected for measurement based on their forecasted development of strong convective conditions. Flight objectives were met though continuous in-flight navigation based on real-time storm development. In June of 2022, two unique thunderstorms near Houston, Texas were measured. This section describes the aspects of the flights that are relevant to the collection of airborne lightning data and includes a map of the NRC Convair-580 flight path, altitude, and the flash distances. WX-500 data were collected continuously throughout the duration of each flight.

The ESCAPE Convair-580 Flight 4 (hereafter CRF4) occurred on June 4th, 2022 between 19:00 and 23:00 UTC and measured the lightning produced by a convective storm system that formed to the west of the Greater Houston Area and about 93 km inland from the coast. The storm developed rapidly around 19:00 UTC and grew towards the coastline until dissipating around 02:00 UTC (∼7 hrs total duration). The NRC Convair-580 was airborne for four hours sampling the atmospheric conditions in and around the storm. Fig. 1b shows the spatial distribution of flashes around the aircraft relative to its flight pattern. Several electrically active cells <10 km wide with relatively low flash production were scattered to the north / east of the aircraft's flight path (S.I. Fig. 2 shows four examples of the spatial distribution of flashes around the aircraft throughout CRF4). The flight path was dominated by long, straight passes that were oriented normal to the main storm system and spiral maneuvers that were used to change altitude. The WX-500 detection range encircles ∼92 %, and the HLMA encircles ∼85 % of the flashes detected by GOES-GLM which has widespread coverage beyond the area of interest. These near equivalent coverages permit the direct comparison of the WX-500 to the HLMA, which is valuable because the HLMA network has superior location accuracy and detection efficiency.

The HLMA detected 22,152 flashes within range of the WX-500. Relative to the NRC Convair-580 heading at the time of measurement, fifty-seven percent of the flashes had a bearing angle direction that fell within the front quadrant (315° to 45°) or rear quadrant (135° to 225°) of the aircraft. Ninety percent of flashes occurred between the distances of 43 km and 167 km from the aircraft, with an average distance of 94 km.

The ESCAPE Convair-580 Flight 12 (hereafter CRF12) took place between 20:46 UTC on June 16th and 00:41 UTC on June 17th and collected data along the western boundary of the storm that produced substantial and widespread lightning over a large area to the east of Houston. The flight path in Fig. 2b was dominated by short passes oriented in all directions and by spiral maneuvers. Fig. 2b shows how flashes were mostly contained within north-east / south-east quadrant relative to the average location (see S.I. Fig. 3 for four examples of the spatial distribution of flashes around the aircraft throughout CRF12). Fig. 2b also shows that WX-500 and HLMA coverage areas do not fully overlap during CRF12. Approximately 40 % of flashes that were within range of the WX-500 were outside the range of the HLMA. Therefore, the GOES-GLM must be used in place of the HLMA to analyze WX-500 performance (when applicable).

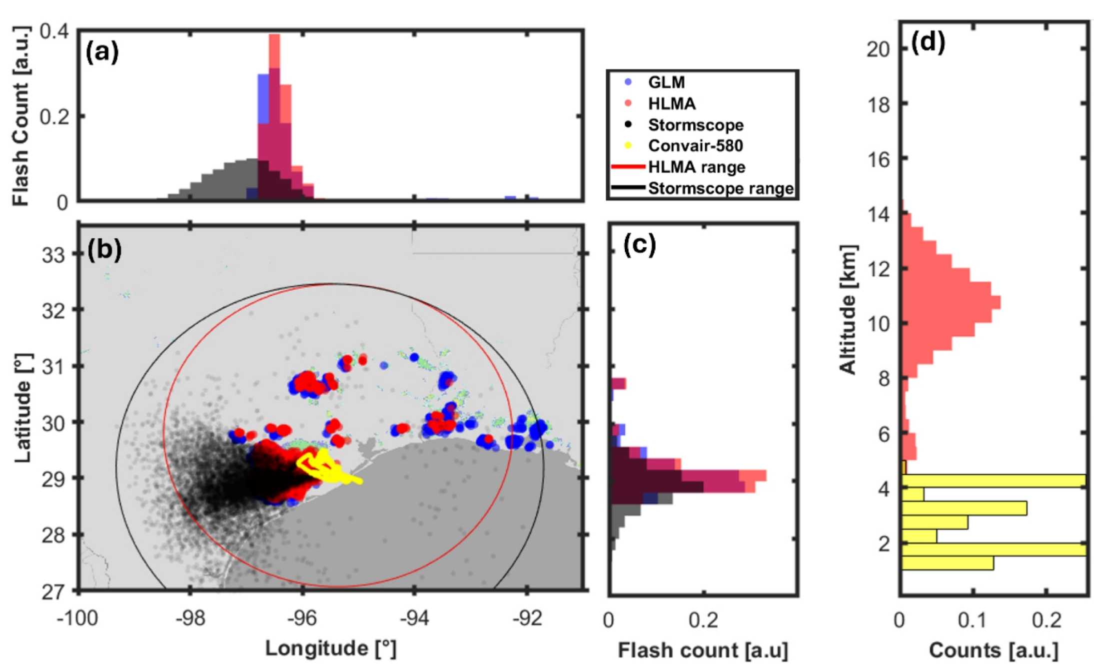

Fig. 1. Plots of CRF4 data showing the: (a) distribution of lightning flashes in the longitudinal direction; (b) map of lightning flashes and NRC Convair-580 flight path from 19:00 to 23:00 UTC on June 4th; (c) distribution of lightning flashes in the latitudinal direction; and (d) distribution of lightning flashes (red) and NRC Convair-580 (yellow) in the vertical direction.

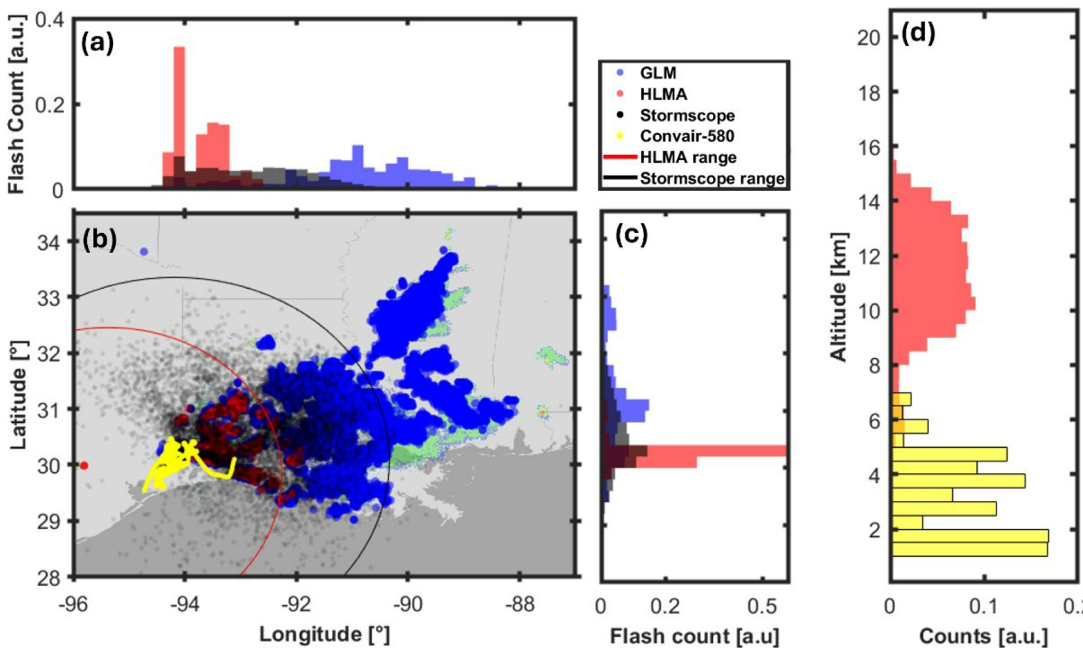

Fig. 2. Plots of CRF12 data showing the: (a) distribution of lightning flashes in the longitudinal direction; (b) map of lightning flashes and Convair-580 flight path from 20:46 to 00:41 UTC on June 16 - 17th; (c) distribution of lightning flashes in the latitudinal direction; and (d) distribution of lightning flashes (red) and Convair-580 (yellow) in the vertical direction.

The GOES-GLM detected 27,672 flashes within range of the WX-500. Relative to the NRC Convair-580 heading at the time of measurement, forty-seven percent of the flashes had a bearing angle direction that fell within the front or rear quadrants of the aircraft. Ninety percent of the detectable GOES-GLM flashes were within 35 km to 363 km of the NRC Convair-580, with a mean flash distance of 250 km (the distribution is skewed towards shorter distances).

2.3. Data preparation and analysis

The authors did not have access to raw or intermediate data products because the algorithm used by the WX-500 to process waveforms is proprietary. The general description of WX-500 signal processing is presented in S.I. Section 3 was gleaned from U.S. Patents 5295,071, 5295,072, and 5537,318, which were assigned to the WX-500 manufacturer prior to its initial release date [20,21,35]. S.I. Section 3 describes how the WX-500: i) processes a measured signal; ii) calculates the range and bearing of the signal's origin for "Strike mode"; and iii) clusters Strike Mode data points by modifying their range to reduce radial spread and to better indicate the expected location of thunderstorm cells to produce "Cell mode" data. Section S.I. 4 describes how measurements were corrected for site error which is a function of antenna location and aircraft shape [36]. Unless otherwise stated, the results in this study were obtained using Cell mode data.

To standardize lightning data for analysis, individual flashes from the HLMA / GOES-GLM and the CG flashes from the NLDN were binned based on their mean flash times to align with the 2 s wide 'lightning-bins' of the WX-500. All flashes within a lightning-bin were re-tagged with the time defined by the right bin edge. When higher integration times were considered, all data were re-processed using wider lightning-bins (e.g., 30, 60, 120, and 300-s). In the context of this work, integration time refers to the interval of time in which data is allowed to continuously populate the flight deck display before the pilot chooses to manually clear the display. Clearing the display regularly allows the pilot to more clearly observe real-time lightning locations and flash rate trends.

To obtain estimates for detection efficiency (i.e., the ability to detect IC and CG flashes) all lightning-bins with *at least* one flash were classified by flash type (HLMA flashes were used for CRF4 and GOES-GLM flashes for CRF12). A lightning-bin was classified as having a CG flash if a coincident return stroke was detected by the NLDN, and as having only IC flashes otherwise. A classified lightning-bin that contained *at least* one WX-500 strike was considered a successful detection. Lightning-bins are classified this way because the WX-500 is most likely to proceed with processing a relatively high intensity signal emitted by a CG flash when an IC and CG flash occurs together. To compare trends in the detection-count over time (i.e., the flash rate) for each lightning mapper, the number of detections per lightning-bin were smoothed using the LOESS method with a span factor of 0.05 [37] and the resulting curves were normalized. Data from CRF4 and CRF12 were used in this analysis.

To investigate the accuracy of lightning locations, bearing and range of the centroid lightning position was calculated for each 2-s lightning-bin. A geospatial filter was applied to ensure that all flashes within a lightning-bin had originated from roughly the same location (i.e., a single storm cell), rather than multiple different locations around the aircraft (i.e., from multiple storm cells). This ensures that centroids were not calculated when, e.g., flashes are produced by two storm cells positioned on opposite sides of the aircraft. The filter eliminated any lightning-bin which contained an HLMA flash that was spread more than 30 km away from the centroid (the average distance from the centroid is called 'centroid distance'). The filter also eliminated any lightning-bin that contained *less than* two WX-500 strikes to reduce the chance of including an erroneous measurement that could have been produced by noise. Since high spatial accuracy is required for this analysis, only the data from CRF4 were used to compare the WX-500 to the HLMA. All variance is reported at 1σ.

Bearing span was used to demonstrate how the WX-500 can accurately capture the range of headings that bound lightning activity to help circumnavigate a thunderstorm. The bearing span is the angular difference between the max and min bearing of WX-500 strikes or HLMA / GOES-GLM flashes. Bearing span is calculated for each lightning-bin. GOES-GLM data was included in this analysis despite its limited spatial accuracy because the purpose of bearing span is to depict the general region that contains lightning activity.

3. Results and discussion

3.1. Lightning detection

3.1.1. Detection efficiency

Table 1 shows the WX-500 detection efficiencies that were measured during CRF4 and CRF12. The WX-500 successfully detected the presence of lightning on more than half of occasions which is demonstrated by the total flash detection efficiency of 53 % and 59 % for CRF4 and CRF12, respectively. As was expected, the WX-500 was much better at detecting lightning given the opportunity to measure a CG flash. The detection efficiency for lightning-bins with a CG flash was 42 % and 22 % greater than without, for CRF4 and CRF12, respectively. Intracloud flashes are more difficult for the WX-500 to detect for several reasons including how: i) their emission peaks at a relatively high frequencies (VFH range) and relative low signal amplitude; ii) they can discharge at high altitudes (and therefore farther distances); and iii) their lightning channels can be non-vertical and follow long meandering routes through the atmosphere (leading to a convoluted waveform that lacks a strong, distinct feature). On the other hand, CG flashes are detected more often because they emit a relatively strong signal and, since lightning channel is linear and vertically oriented especially near the earth's surface, they generate a more consistent and distinct waveform that aids in signal processing [38].

Table 1 shows the WX-500 detection efficiency for IC flashes was relatively low at 33 % and 42 % for CRF4 and CRF12, respectively. Failing to detect IC flashes on more than half of occasions can be concerning for several reasons including how IC flashes: i) are not always accompanied by a CG flash which had detection rates of 75 % and 64 % for CRF4 and CRF12, respectively; ii) can occur several kilometers away from CG flashes; iii) can occur at rates of 2 × to 10 × that of CG discharges [39–41]; and iv) pose a direct threat to airborne operations. This demonstrates why it is important to further improve WX-500 performance. On the other hand, comparisons to NLDN performance show that detecting every IC flash is not essential to constitute an informative lightning mapper. The NLDN has been providing comprehensive lightning data for over 40 years while operating with an estimated IC flash detection efficiency between 16 % to 38 % before network upgrades in 2013 added TOA processing techniques [42] that improved levels to between 30 % to 58 %. Therefore, simply detecting *that* lightning is nearby, or providing an accurate *trend* of lightning production, can be an adequate warning of lighitng activity. This is discussed further in Section 3.1.2.

The results in Table 1 agree well across flights given how the detection efficiencies for IC, CG, and total flashes differ by no more than 11 %. Some disagreement across flight test results is always expected since no two thunderstorms are the same (i.e., the distribution of flash powers and the spatial distribution of flashes relative to the aircraft location will always be unique). The use of two different detection methods as sources for validation datasets also contributes to this disagreement and is a likely explanation for the slight improvement in the detection efficiency of IC and total flashes observed during CRF12. The WX-500 is expected to agree more closely with GOES-GLM because both instruments tend to capture the most powerful flashes, or in other words, the flashes with larger peak currents that produce hotter and brighter channels that are more visible to the satellite [33]. Given how influential certain factors can be on the detection efficiency (e.g., flash power, distance, type), the general agreement across Table 1 suggests these results might apply reasonably well to the average WX-500 thunderstorm measurement.

3.1.2. Flash rate

Fig. 3a shows the smoothed and normalized flash rate curves from CRF4. Although the first WX-500 detections were slightly delayed (by 3 mins and 44 s after the first HLMA detection at 19:03:01 UTC), results in Fig. 3a show the WX-500 flash rate tracks well with the other measurements, providing adequate warning of lightning activity throughout the entire flight. The WX-500 was able to capture the gradual increase in flash rate over time, despite only having a total detection efficiency of around 50 %, because the temporal distribution of flashes that went undetected were nearly proportional to those that were detected. Since IC and CG flash distributions were proportional to one another during CRF4, as demonstrated by the comparable green (CG) and the red curves (CG + IC) in Fig. 3a, having a poor detection efficiency for IC flashes did not affect the results. While this may not be the case for every thunderstorm, this explains how the WX-500 can capture accurate lightning trends despite being weakly sensitive to IC flashes.

There were two major departures from the general trend that occurred at 20:26 and 21:03 UTC and are pointed out by the olive-colored arrows in Fig. 3a and b. The arrows show how the artificial surges in flash rate mirror the sudden reductions in flash distance, which is caused by the NRC Convair-580 heading towards and then turning away from the active lightning area. Due to the inverse square law, the WX-500 will become more sensitive to the weaker flashes as the lightning draws nearer or the aircraft is approaching a storm cell. The WX-500 proved capable of detecting flash powers as low as 5e-5 to 1e-4 dBW at 75 to 130 km (individual detections of two CG flashes and one IC flash), but more WX-500 measurements are needed to further investigate sensitivity across its working range. While beneficial in terms of flight safety (because the chances of detecting lightning improve as the storm approaches), variations in WX-500 sensitivity force pilots to consider flight track history (relative to the storm location) when using flash rate trends to infer whether a storm is building, maturing, or dissipating.

3.2. Lightning mapping

3.2.3. Mapping accuracy

The x-axis in Fig. 4 shows the distribution of WX-500 bearing errors from CRF4. Results show WX-500 Cell mode was within $\pm 14^{\circ}$ and Strike mode was within $\pm 17^{\circ}$ of the true flash bearing, with neither mode showing any observable bias. Further testing revealed that increasing the integration time from 2 to 30 s improved the precision of Cell mode to $\pm 4^{\circ}$ ($n = 62$) and Strike mode to $\pm 8^{\circ}$ ($n = 70$) when obvious outliers were ignored (e.g., bearing errors > $|50^{\circ}|$). Using Cell mode, thirty-two individual CG flashes were measured to within $\pm 7^{\circ}$ of their true bearing and seventy-two IC flashes were within $\pm 8^{\circ}$, respectively. A two sample F-test for variance was used to compare the error distributions when measuring the individual IC and CG flashes which determined that flash type does not have a statistically significant influence on bearing.

Table 1
WX-500 detection efficiency of IC and CG lightning bins considering multi-flash lightning-bins from CRF4 and CRF12.

Flight	CRF4		CRF12	
Total # of 2-s Detection Windows	6364 (HLMA)		7052 (GOES-GLM)	
	Bins With ≥1 Flash	and ≥1 WX-500 Strike	Bins With ≥1 Flash	and ≥1 WX-500 Strike
IC	2935	978 (33 %)	1485	616 (42 %)
CG	2537	1944 (75 %)	4382	2814 (64 %)
Total	5472	2922 (53 %)	5840	3430 (59 %)

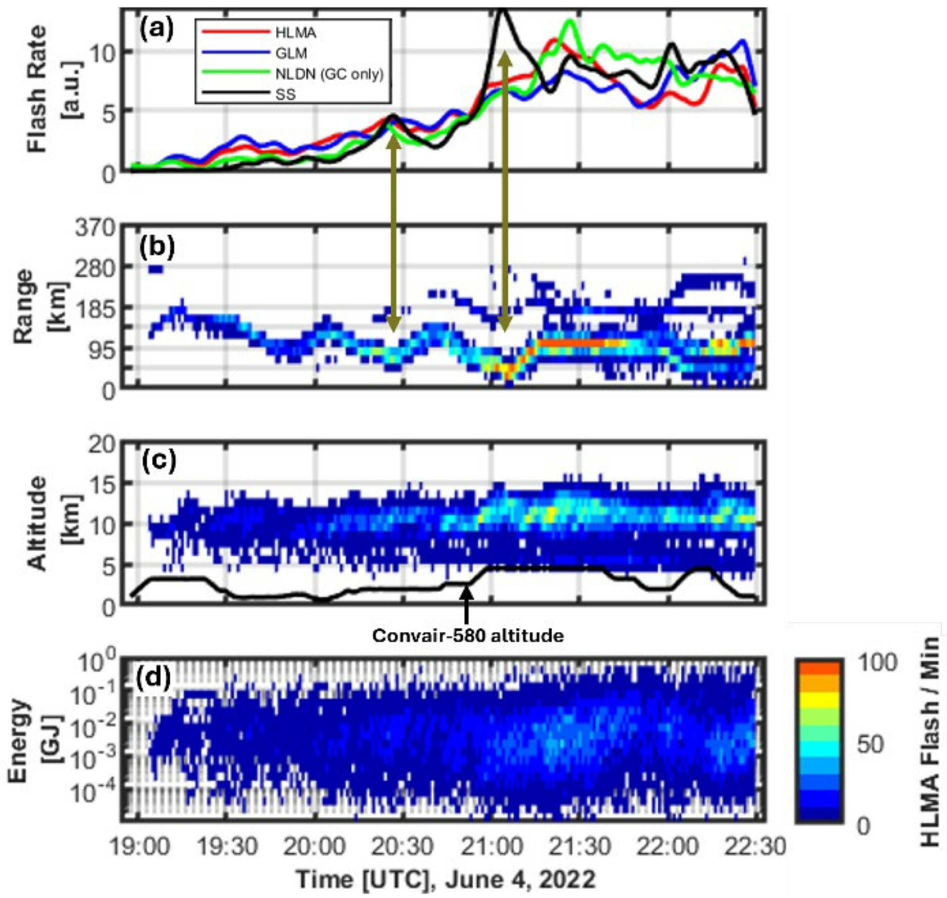

Fig. 3. Plots of CRF4 data showing the: (a) time-series flash rate curves smoothed using the LOWESS method and a span factor of 0.05; (b) heatmap of flash distance; c) heatmap of flash altitude; and (d) heatmap of flash energy.

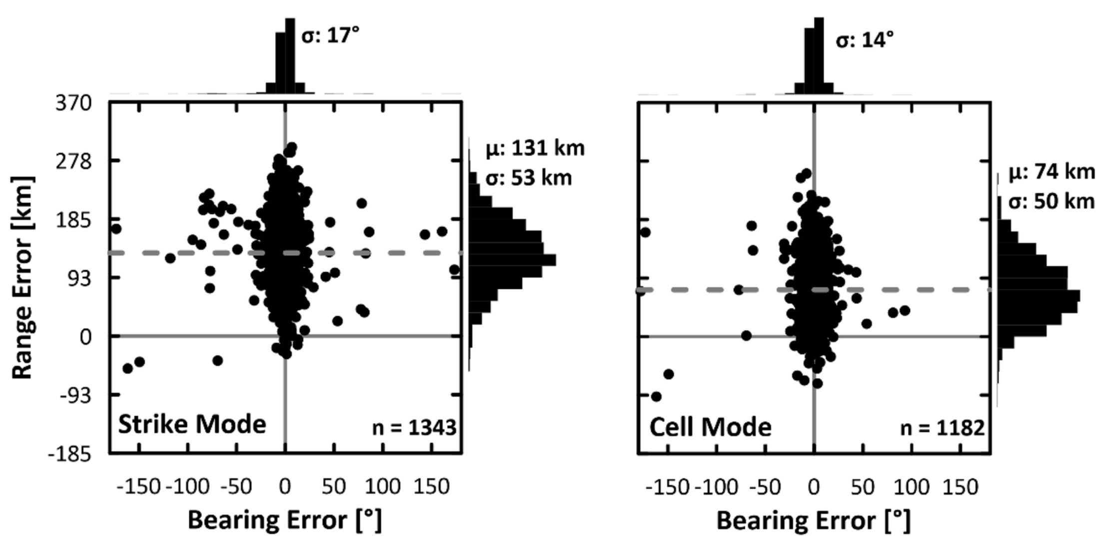

Fig. 4. Scatter plot of CRF4 data showing the WX-500 bearing and range error distributions for Strike mode (left) and Cell mode (right).

Results demonstrating that the WX-500 bearing has a reasonable level of precision were expected since the original Ryan Stormscope was shown to have a precision of ±13° in the work of Baum and Seymour (1980) (they analyzed eight individual storm passes lasting upwards of 5 mins each with no lightning-bin discretization and a cluster filter that removed outliers [16,43]).

The y-axis in Fig. 4 shows the distribution of WX-500 range errors from CRF4. Results show that range was consistently overpredicted by an average of +74 km (±50 km) for Cell mode and +131 km (±53 km) for Strike mode. Further reducing integration time reduces the variance between measurements, but does not reduce the overprediction bias of the instrument below +74 km. This level of bias is considerable given that the average true flash distance from CRF4 was 94 km. Combining data from both flights suggest that on average, the WX-500: i) overpredicts when true flash distance is at ¼ full measurement range; ii) has minimal bias around ½ full measurement range; iii) underpredicts around ¾ full measurement range; and iv) has large variance across the entire measurement range. Radial spreading or spoking is a well-known artifact of the WX-500 because it infers range from measured signal intensities, which is even depicted in the user manual [22]. The spoking effect could have been exacerbated during these flights because flash power was highly variable (e.g., Fig. 3d shows flash energy spanned 5 orders of magnitude during CRF4), and it is possible that potential signal interference from the many experimental probes and sensors equipped onboard the NRC Convair-580 could have compounded any measurement errors. Despite these range errors (the possible improvement of which is discussed in Section 3.3), the WX-500 can still provide accurate spatial information about lightning activity through bearing span.

3.2.4. Bearing span

Fig. 5a shows a typical example of WX-500 bearing span covering nearly the entire region of lightning activity over a 2-min interval during CRF12. Here, the WX-500 boundaries establish the interval of headings that point towards lightning activity, which is sufficient to circumnavigate the storm despite inaccuracies in the radial positioning of strikes. Fig. 5a, b, and c show how correlation between the WX-500 and GOES-GLM bearing span improves as integration time grows, up to around 1 min, above which there is little improvement. In practice, pilots should allow WX-500 data to populate their screen for at least 1 min before using the lightning boundaries as a navigational aid. Further testing indicated that when large differences in lightning rate exist between two distant storm cells (e.g., CRF4, which had stronger activity to the west and weaker activity to the east), the WX-500 can have difficulty distinguishing whether the signals from the weak cell are truly flashes or just noise. Nonetheless, bearing span can provide valuable weather information to pilots who don't have access to on-board weather radar and at better refresh rates than streaming services. Bearing span can help pilots to locate thunderstorm cells when radar products are not available.

3.3. Comments on future work

The distribution of data about the y-axis in Fig. 6 shows how Cell mode data was more tightly clustered than Strike mode during CRF4. The distribution of data about the x-axis in Fig. 6 shows that the Cell mode centroid was a more accurate estimate of the true flash centroid location than Strike mode during CRF4. Since Cell mode is an improvement over Strike more, but does not completely fix the spoking errors, there is a clear opportunity to further develop the airborne lightning mapper. Future work to improve ranging estimates should consider using a combination of several ranging techniques to estimate distance including the: i) measured signal intensity; ii) ratio of the electric and magnetic components; iii) ratio of magnetic components at multiple frequencies; and iv) intensity of electric components in two orthogonal planes [44]. Additional single-station ranging techniques with location errors of less than 10 % could be adapted for airborne use

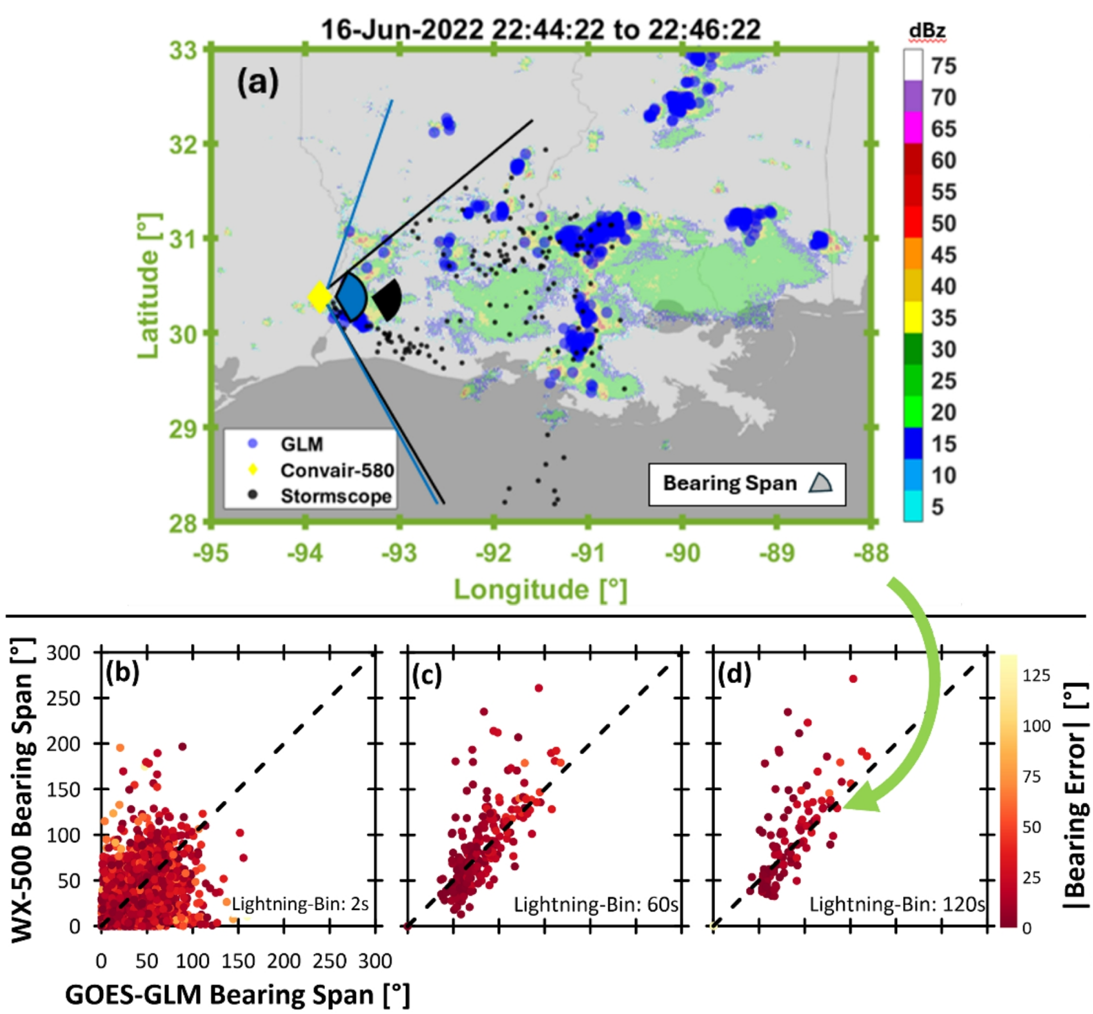

Fig. 5. Plots of CRF12 data showing: (a) a map of lightning activity over a 2-min interval with graphics that depict bearing span and lightning bounds; and the correlations between the bearing span of the GOES-GLM and WX-500 for integration times of (b) 2 s, (c) 60 s, and (d) 120 s.

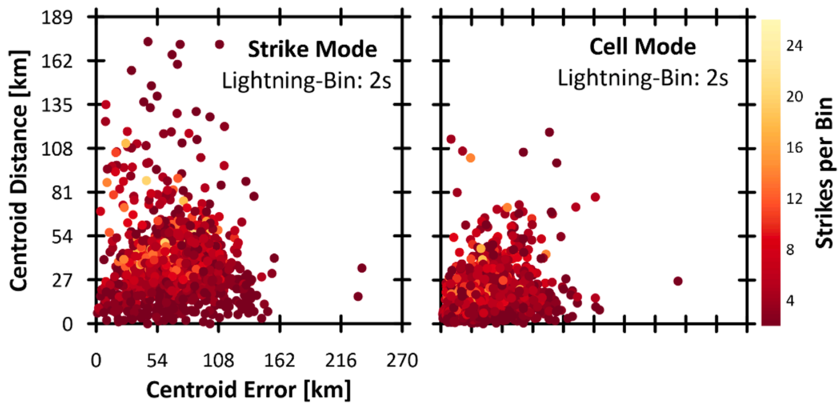

Fig. 6. Plots of CRF4 data comparing the location error of the WX-500 centroid (x-axis) and the WX-500 cluster compactness (y-axis) between Strike and Cell modes.

including the work by Ramachandran et al. (2007) who used the period and delay from the waveform of the electric field to infer distance [45], or the work by Koochak and Fraser-Smith (2019) who used the VLF and ELF components of the electromagnetic signal to infer range [46].

Future work should record raw waveforms along with the collocated data from a VHF network and the NLDN to develop advanced algorithms that distinguish between IC and CG flashes and inform pilots as to which type of flash is nearby. Advanced clustering algorithms that further reduce the radial spread of individual strikes should also be investigated. These algorithms should use advanced statistical methods to locate individual storm cells and should correct the location of older strikes as more data becomes available. Airborne lightning mappers like the WX-500 and the Honeywell LSZ-860 simply overlay lightning data onto existing radar products and advanced radar systems like the RDR-400 Honeywell weather radar [47] claim to predict lightning before it occurs but do not measure it directly. Therefore, future work should fuse radar data with lightning data to provide a superior radar product that can clearly identify thunderstorm cells to reduce the cognitive load on the pilot.

4. Conclusions

A Stormscope Weather Mapping System (WX-500 Series 2) was installed on the NRC Convair-580 research aircraft and used to measure lightning activity during the only two thunderstorm flights of the ESCAPE campaign near Houston, TX, in 2022. The airborne lightning measurements were collocated with the Houston Lightning Mapping Array, the National Lightning Detection Network, and the GOES – Geostationary Lightning Mapper. The WX-500 had detection efficiencies of 33 % and 42 % for intracloud flashes, 75 % and 64 % for cloud to ground flashes, and 53 % and 79 % for total flashes. The bearing direction to lightning activity (relative to aircraft heading) was accurate to within $\pm 14^\circ$ (σ), which improved to $\pm 4^\circ$ when integration time was increased from 2 to 30 s and clear outliers were ignored. The range distance to lightning activity was overestimated by an average of 74 km ($\pm$50 km) during a flight with an average true flash distance of 94 km. The WX-500 bearing span was shown to capture the angular boundary of lightning activity at an integration time of 1 min and provides sufficient geospatial lightning information to safely circumnavigate a thunderstorm. Despite the significant bias in the range error of the instrument, Cell mode helped to reduce the radial 'spoke' errors and provides a general improvement over Strike mode. There is clear opportunity to further develop the airborne lightning mapper, whether it be improving the ranging calculation, developing advances statistical clustering methods, or fusing lightning data with on-board weather radar to produce a superior radar product.

Nomenclature

ADS–B, Automatic Dependent Surveillance–Broadcast
CG, Cloud to Ground Flash
CONUS, Continental United States
CRF4, ESCAPE Convair Flight 4
CRF12, ESCAPE Convair Flight 12
DF, Magnetic Direction-Finding
ELF, Extremely Low Frequency
ESCAPE, Experiment of Sea Breeze Convection, Aerosols, Precipitation, and Environment
GOES-GLM, Geostationary Operational Environmental Satellite-Geostationary Lightning Mapper
HLMA, Houston Lightning Mapping Array
IC, Intracloud Flash
NLDN, National Lightning Detection Network
NRC, National Research Council of Canada
RPAS, Remotely Piloted Aircraft Systems
TOA, Time of Arrival
UAV, Unmanned Aerial Vehicles
VHF, Very High Frequency
VLF, Very Low Frequency
VTOL, Vertical Take-Off and Landing aircraft

Data availability

WX-500 data will be made available upon request. NLDN data was provided by Vaisala Inc. and must be acquired through their academic support portal. All other ESCAPE data is publicly available (e.g., see [27])

CRediT authorship contribution statement

Zachary Milani: Writing – original draft, Visualization, Validation, Software, Methodology, Investigation, Formal analysis, Data curation, Conceptualization. **Leonid Nichman:** Writing – review & editing, Supervision, Resources, Investigation, Data curation, Conceptualization. **Edgar Matida:** Writing – review & editing, Supervision, Investigation, Conceptualization. **Liam Fleury:** Writing – review & editing, Validation. **Mengistu Wolde:** Writing – review & editing, Project administration, Funding acquisition. **Eric Bruning:** Writing – review & editing, Project administration, Funding acquisition, Data curation, Conceptualization. **Greg M. McFarquhar:** Writing – review & editing, Project administration, Funding acquisition. **Pavlos Kollias:** Project administration, Funding acquisition.

Declaration of competing interest

The authors declare that they have no known competing financial interests or personal relationships that could have appeared to influence the work reported in this paper.

Acknowledgement

The authors would like to thank the co-PIs of the ESCAPE campaign, weather forecasters, flight crew, and instrumentation and maintenance teams that made the ESCAPE campaign successful. The authors would like to acknowledge the USA National Science Foundation (NSF) grants that made the ESCAPE campaign possible: AGS-2019932 (PK, MO, KL), AGS-2020000 (KL, MK, KM), AGS-2019939 (EB, TL), AGS-2019968 (GMM, AD and SP), AGS-2019947 (SV, BA) and AGS-2019649 (RAS, NA, ER). In addition, the authors would like to acknowledge the support from the U.S. DOE Office of Science Biological and Environmental Research Atmospheric System Research Program (contract DE-SC0012704, DE-SC0021247 and DE-SC0021160 (SV)). The authors would also like to acknowledge the National Research Council of Canada (NRC) Aeronautical Product Development and Certification (APDC) program for funding this analysis. The authors would also like to acknowledge Vaisala Inc. and its Xweather team for providing NLDN data through personal communications. The authors would also like to acknowledge Mathieu Lachapelle for his contributions to this investigation.

Supplementary materials

Supplementary material associated with this article can be found, in the online version, at doi:10.1016/j.ast.2025.110038.

References

[1] M. Ostermann, J. Schodl, P.A. Lieberzeit, P. Bilotto, M. Valtiner, Lightning strike protection: current challenges and future possibilities, Materials. (Basel) 16 (2023) 1743, https://doi.org/10.3390/ma16041743.
[2] B. Wang, Y. Zhu, Y. Ming, X. Yao, X. Tian, G. Ziegmann, Y. Duan, J. Sun, Understanding lightning strike induced damage mechanism of carbon fiber reinforced polymer composites: an experimental study, Mater. Des. 192 (2020), https://doi.org/10.1016/j.matdes.2020.108724.
[3] P. Feraboli, M. Miller, Damage resistance and tolerance of carbon/epoxy composite coupons subjected to simulated lightning strike, Compos. Part a Appl. Sci. Manuf. 40 (2009) 954–967, https://doi.org/10.1016/j.compositesa.2009.04.025.
[4] A. Larsson, The interaction between a lightning flash and an aircraft in flight, C. R. Phys. 3 (2002) 1423–1444, https://doi.org/10.1016/S1631-0705(02)01410-X.
[5] V. Kumar, T. Yokozeki, C. Karch, A.A. Hassen, C.J. Hershey, S. Kim, J.M. Lindahl, A. Barnes, Y.K. Bandari, V. Kunc, Factors affecting direct lightning strike damage to fiber reinforced composites: a review, Compos. B Eng. 183 (2020) 107688, https://doi.org/10.1016/j.compositesb.2019.107688.
[6] C. Kuang, K. Fu, J. Lee, H. Zhu, Q. Shi, X. Cui, Experimental and modelling of lightning damage to carbon fibre-reinforced composites under swept stroke, Coatings 13 (2023) 2048, https://doi.org/10.3390/coatings13122048.
[7] J. McCarthy, R. Serafin, J. Wilson, J. Evans, C. Kessinger, W.P. Mahoney, Addressing the microburst threat to aviation research-to-operations success story, Bull. Am. Meteorol. Soc. 103 (2022) E2845–E2861, https://doi.org/10.1175/BAMS-D-22-0038.1.
[8] T.P. Lane, R.D. Sharman, Intensity of thunderstorm-generated turbulence revealed by large-eddy simulation, Geophys. Res. Lett. 41 (2014) 2221–2227, https://doi.org/10.1002/2014GL059299.
[9] SiriusXM, SiriusXM Aviation, (n.d.). https://www.siriusxm.ca/aviation (accessed January 25, 2025).
[10] R. Still, Practical Meteorology, An Algebra-based Survey of Atmospheric Science -v102b, Univ. of British Columbia, 2017, pp. 481–544, isbn 978-0-88865-283-6.
[11] Extant Aerospace, Extant Aerospace Acquires Stormscope® Product Line from L3Harris, 2019. Melbourne, www.extantaerospace.com.
[12] Honeywell International Inc., LSZ-860 Lightning Sensor System, Pheonix (2006). www.honeywell.com.
[13] Insight Avionics Inc., Strike Finder: Pilots Guide (Revision 2.0), Buffalo, 1997. www.insightavionics.com.
[14] T.D. Crum, R.L. Alberty, The WSR-88D and the WSR-88D Operational Support Facility, Bull. Am. Meteorol. Soc. 74 (1993) 1669–1687, https://doi.org/10.1175/1520-0477(1993)074<1669:TWATWO>2.0.CO;2.
[15] R.E. Orville, Development of the national lightning detection network, Bull. Am. Meteorol. Soc. 89 (2008) 180–190, https://doi.org/10.1175/BAMS-89-2-180.
[16] R.K. Baum, T.J. Seymour, Flight Evaluation of a Severe Weather Avoidance System For Aircraft (AFWAL-TR-80-3022, Flight Dynamics Laboratory (AFWAL), Wright-Patterson AFB, Ohio, 1980.
[17] L.C. Walko, M.J. Reazer, Data Acquisition for Evaluation of an Airborne Lightning Detection System (AFWAL-TR-83-3083), Flight Dynamics Laboratory (AFWAL), Wright-Patterson AFB, Ohio, 1983.
[18] B. Bernstein, S. DiVito, J.T. Riley, S. Landolt, J. Haggerty, G. Thompson, D. Adriaansen, D. Serke, C. Kessinger, S. Tessendorf, M. Wolde, A. Korolev, A. Brown, L. Nichman, D. Sims, C. Dumont, The In-Cloud Icing and Large-Drop Experiment (ICICLE) Science and Operations Plans (DOT/FAA/TC-21/29)," Atlantic City, 2021, https://doi.org/10.21949/1524472.
[19] P. Kollias, G.M. McFarquhar, E. Bruning, P.J. DeMott, M.R. Kumjian, P. Lawson, Z. Lebo, T. Logan, K. Lombardo, M. Oue, G. Roberts, R.A. Shaw, S.C. van den Heever, M. Wolde, K.R. Barry, D. Bodine, R. Bruintjes, V. Chandrasekar, A. Dzambo, T.C.J. Hill, M. Jensen, F. Junyent, S.M. Kreidenweis, K. Lamer, E. Luke, A. Bansemer, C. McCluskey, L. Nichman, C. Nguyen, R.J. Patnaude, R.J. Perkins, H. Powers, K. Ranjbar, E. Roux, J. Snyder, B.P. Treserras, P. Tsai, N.A. Wales, C. Wolff, N. Allwayin, B. Ascher, J. Barr, Y. Hu, Y. Huang, M. Litzmann, Z. Mages, K. McKeown, S. Patil, E. Rosky, K. Tuftedal, M.-D. Tzeng, Z. Zhu, Experiment of sea breeze convection, aerosols, precipitation and environment (ESCAPE), Bull. Am. Meteorol. Soc. (2024), https://doi.org/10.1175/BAMS-D-23-0014.1.
[20] J.G. Kuzma, B.M. Stevens, Sampled data lightning strike detection and mapping system capable of generating frequency spectrum of input signal waveforms and displaying such on the mapping display, US Patent 5 (295) (1994) 071.
[21] B.M. Stevens, J.G. Kuzma, Sampled data lightning strike detection and mapping system capable of recovering a pre threshold sample history for detection and mapping processing, US Patent 5 (295) (1994) 072.
[22] BFGoodRich Avionics Systems Inc, User's Guide WX-500 Stormscope Series II Weather Mapping Sensor ® Users Guide, Grand Rapids, 1997.
[23] T. Logan, An analysis of the performance of the houston lightning mapping array during an intense period of convection during tropical storm harvey, J. Geophys. Res.: Atmosph. 126 (2021), https://doi.org/10.1029/2020JD033270.
[24] E.C. Bruning, K.N. Brunner, M. van Lier-Walqui, T. Logan, T. Matsui, Lightning and radar measures of mixed-phase updraft variability in tracked storms during the TRACER field campaign in houston, texas, Mon. Weather. Rev. 152 (2024) 2753–2769, https://doi.org/10.1175/MWR-D-24-0060.1.
[25] M.R. Cullen, The Houston Lightning Mapping Array: Network and Installation and Preliminary Analysis, Texas A&M University, 2013. MSc thesis.
[26] V.C. Chmielewski, E.C. Bruning, Lightning Mapping Array flash detection performance with variable receiver thresholds, J. Geophys. Res. 121 (2016) 8600–8614, https://doi.org/10.1002/2016JD025159.
[27] Timothy Logan, Eric Bruning, Kelcy Brunner, Jessica Souza, Houston lightning mapping array (HLMA) Flash-level data, UCAR/NCAR, Earth Obser. Laborat. (2023), https://doi.org/10.26023/GBKS-E7VT-HS11 (accessed June 26, 2024).
[28] A. Nag, M.J. Murphy, K.L. Cummins, A.E. Pifer, J.A. Cramer, Recent Evolution of the U.S. national lightning detection network, in: 23rd Int. Lightning Detection Conf./Fifth Int. Lightning Meteorology Conf., Vaisala, Tuscon, AZ, 2014. https://www.vaisala.com/sites/default/files/documents/Nag%20et%20al-Recent%20Evolution%20of%20the%20U.S.%20National%20Lightning%20Detection%20Network-2014-ILDC-ILMC.pdf (accessed August 28, 2024).
[29] M.J. Murphy, A. Nag, J.A. Cramer, A.E. Pifer, Enhanced cloud lightning performance of the U.S. National Lightning Detection Network following the 2013 upgrade, in: 23rd Int. Lightning Detection Conf./Fifth Int. Lightning Meteorology Conf., Vaisala, Tuscon, AZ, 2014. https://www.vaisala.com/sites/default/files/documents/Murphy%20et%20al-Improved%20NLDN%20Performance%20after%202013%20Upgrade-2014-ILDC-ILMC.pdf (accessed August 28, 2024).
[30] S. Mallick, V.A. Rakov, J.D. Hill, T. Ngin, W.R. Gamerota, J.T. Pilkey, C.J. Biagi, D. M. Jordan, M.A. Uman, J.A. Cramer, A. Nag, Performance characteristics of the NLDN for return strokes and pulses superimposed on steady currents, based on rocket-triggered lightning data acquired in florida in 2004–2012, J. Geophys. Res. 119 (2014) 3825–3856, https://doi.org/10.1002/2013JD021401.
[31] C.J. Biagi, K.L. Cummins, K.E. Kehoe, E.P. Krider, National lightning detection network (NLDN) performance in southern Arizona, Texas, and Oklahoma in 2003-2004, J. Geophys. Res. Atmosph. 112 (2007), https://doi.org/10.1029/2006JD007341.
[32] S.J. Goodman, R.J. Blakeslee, W.J. Koshak, D. Mach, J. Bailey, D. Buechler, L. Carey, C. Schultz, M. Bateman, E. McCaul, G. Stano, The GOES-R Geostationary Lightning Mapper (GLM), Atmos. Res. 125–126 (2013) 34–49, https://doi.org/10.1016/j.atmosres.2013.01.006.
[33] D. Zhang, K.L. Cummins, Time Evolution of Satellite-Based Optical Properties in Lightning Flashes, and its Impact on GLM Flash Detection, J. Geophys. Res. Atmosph. 125 (2020), https://doi.org/10.1029/2019JD032024.
[34] NOAA, Geostationary Operational Environmental Satellites (GOES) 16, 17 & 18, (n.d.). https://data.eol.ucar.edu/dataset/100.037 (accessed April 24, 2024).
[35] R.L. Moses, J.G. Kuzma, K.A. Ostrander, B.M. Stevens, all of Ohio, Lightning strike detection and mapping system, US Patent 5 (537) (1996) 318.
[36] L. Parker, H. Kasemir, Airborne Warning Systems for Natural and Aircraft-Initiated Lightning, IEEE Trans Electromagn Compat EMC-24 (1982) 137–158, https://doi.org/10.1109/TEMC.1982.304009.
[37] W.S. Cleveland, S.J. Devlin, Locally Weighted Regression: an Approach to Regression Analysis by Local Fitting, J. Am. Stat. Assoc. 83 (1988) 596–610, https://doi.org/10.1080/01621459.1988.10478639.
[38] E.P. Krider, R.C. Noggle, A.E. Pifer, D.L. Vance, Lightning Direction-Finding Systems for Forest Fire Detection, Bull. Am. Meteorol. Soc. 61 (1980) 980–986, https://doi.org/10.1175/1520-0477(1980)061/3C0980:LDFSFF/3E2.0.CO;2.

[39] K.L. Cummins, M.J. Murphy, An overview of lightning locating systems: history, techniques, and data uses, with an in-depth look at the U.S. NLDN, IEEe Trans. Electromagn. Compat. 51 (2009) 499–518, https://doi.org/10.1109/TEMC.2009.2023450.

[40] V.A. Rakov, Electromagnetic methods of lightning detection, Surv. Geophys. 34 (2013) 731–753, https://doi.org/10.1007/s10712-013-9251-1.

[41] E.P. Krider, R.C. Noggle, A.E. Pifer, D.L. Vance, Lightning direction-finding systems for forest fire detection, Bull. Am. Meteorol. Soc. 61 (1980) 980–986, https://doi.org/10.1175/1520-0477(1980)061<0980:LDFSFF>2.0.CO;2.

[42] M.J. Murphy, J.A. Cramer, R.K. Said, Recent History of Upgrades to the U.S. National Lightning Detection Network, J. Atmos. Ocean. Technol. 38 (2021) 573–585, https://doi.org/10.1175/JTECH-D19-0215.1.

[43] T.J. Seymour, R.K. Baum, Evaluation of the Ryan Stormscope As a Severe Weather Avoidance System For Aircraft Preliminary Report (Rep. FAA-RD-79-6), 1979. Melbourne, FL.

[44] F.J. Yanovsky, A. Korablev, Airborne sensor for passive determination of the distance up to lightning source, IGARSS 2000. IEEE 2000 International Geoscience and Remote Sensing Symposium. Taking the Pulse of the Planet: The Role of Remote Sensing in Managing the Environment. Proceedings (Cat. No.00CH37120) 7 (n.d.) 3172–3174. https://doi.org/10.1109/IGARSS.2000.860373.

[45] V. Ramachandran, J.N. Prakash, A. Deo, S. Kumar, Lightning Stroke Distance Estimation From Single Station Observation and Validation With WWLLN Data, Ann. Geophys. 25 (2007) 1509–1517, https://doi.org/10.5194/angeo-25-1509-2007.

[46] Z. Koochak, A. Fraser-Smith, Single-Station Lightning Location Using Azimuth and Time of Arrival of Sferics, Radio Sci. 55 (2020), https://doi.org/10.1029/2018RS006627.

[47] Honeywell International Inc., IntuVue (RDR-4000) Weather Radar, Pheonix (2015).